PHYSICAL REVIEW E VOLUME 59, NUMBER 2 FEBRUARY 1999

Comparison of critical properties in binary and ternary liquid mixtures using light scattering techniques

O. Müller and J. Winkelmann*
Institut für Physikalische Chemie, Universität Halle-Wittenberg, Geusaer Strasse, D-06217 Merseburg, Germany

(Received 24 October 1997; revised manuscript received 15 October 1998)

In this paper we present results of light scattering and viscosity measurements of both binary and ternary mixtures. The investigations are carried out for two liquid systems: aniline+cyclohexane and aniline+cyclohexane+p-xylene. Correlation lengths, generalized osmotic susceptibilities, mutual diffusion coefficients, and viscosities are obtained for a range of compositions and temperatures where the systems becomes nearly critical. We investigate the shift in critical exponents, the validity of power laws, and the role of corrections to scaling when we change from a binary critical point to a ternary plait point. It is shown that critical exponents of the ternary mixture, obtained from power-law fitting, are apparently larger than those of a binary mixture. A possible influence of corrections to scaling on the critical behavior of a ternary mixture is discussed. [S1063-651X(99)04502-X]

PACS number(s): 05.70.Jk

I. INTRODUCTION

Static and dynamic light scattering measurements have proved to be powerful techniques for studying critical phenomena in fluid phases. The angle-dependent intensity and the spectrum of scattered light can be easily related to the magnitude and the dynamics of critical fluctuations [1,2]. Many papers published in recent decades are concerned with the analysis of these long-range correlations in binary systems in the neighborhood of their plait points (e.g., the aniline+cyclohexane system [3–6]). It could be shown that theoretical concepts such as renormalization group or mode-mode coupling theory are in impressive agreement with the results of measurements in binary fluid mixtures. In a three-component system one could expect that the plait point should behave analogously to the critical mixing point of a two-component system. However, there is in fact an important difference in the case of a ternary plait point: Under constant pressure it is a part of a critical line on a coexistence surface. There are only a few papers that deal with the critical behavior in three component critical fluids. Bak and Goldburg [7] observed no change in the critical exponent of osmotic susceptibility when they add up to 6% phosphoric acid to a critical mixture of water and phenol. In contrast to this result, a mixture of brombenzene, water, and acetone gave a critical exponent that was larger than the binary one [8]. Fisher and Scesney explained this trend by renormalization of critical exponents from analysis of the free-electron Ising model [9,10], e.g.,

$$\nu_x = \frac{\nu}{1-\alpha}, \qquad \gamma_x = \frac{\gamma}{1-\alpha}, \tag{1}$$

where ν is the critical exponent of the correlations length of concentration fluctuations ξ, γ denotes the exponent of the generalized osmotic susceptibility $C\chi$, and α is the heat capacity exponent above the plait point. The subscript x denotes that this quantity is an exponent of a ternary plait point.

In an extended investigation of the ethanol-water-chloroform system Chu and Lin [11] found larger exponents for the correlation length and the osmotic susceptibility than expected by critical exponent renormalization. Because of this situation it becomes necessary to study the nature of critical anomalies in three-component systems. The existence of a critical line leads to the assumption that in a ternary mixture values of critical exponents may be found in a certain range instead of being fixed as in a binary mixture. The exponents of the binary system should be a limit to this range.

In the first step of this systematic study we intend to perform a direct comparison of a binary and a ternary fluid system. These systems should differ only by the third component. For this purpose we measured a critical mixture of aniline and cyclohexane and afterward we performed exactly the same measurements with a critical ternary mixture of aniline, cyclohexane, and p-xylene. The refractive index n_D of p-xylene corresponds to the refractive index of the binary critical mixture. So the presence of p-xylene has no influence on optical properties of the system.

II. THEORY

A. Intensity of scattered light

Light scattering can be observed whenever there are local fluctuations in the dielectric constant ε of the medium. The intensity I_s of the scattered light is given by

$$I_s(q) = A \sin^2(\Phi)\langle|\delta\varepsilon(q)|^2\rangle \tag{2}$$

from the static point of view. In this equation A denotes a constant determined by the wavelength λ of incident beam. Φ is the phase shift between the incident and the scattered beam, and q is the so-called wave vector. It is defined by

---

*Author to whom correspondence should be addressed. FAX: +49-3461-46-2129.
Electronic address: winkelmann@chemie.uni-halle.de

$$q=4\pi\frac{n_D}{\lambda^4}\sin\left(\frac{\theta}{2}\right), \tag{3}$$

with the scattering angle θ and the refractive index n_D. In a fluid mixture the local fluctuations of the dielectric constant are a function of fluctuations in pressure p, temperature T, and concentration c. Under the given conditions the concentration fluctuations are doubtlessly much more essential than the others. So we can formulate the scattered intensity as

$$I_s(q)=A\sin^2\left(\frac{\partial\epsilon}{\partial c}\right)^2_{p,T}\langle|\delta c(q)|^2\rangle. \tag{4}$$

The quantity $\langle|\delta c(q)|^2\rangle$, describing the concentration fluctuations in space, is the static structure factor $S(q)$. It is strongly connected to the space autocorrelation function of the concentration fluctuations $G(r)$,

$$S(q)=V\int_V e^{iqr}G(r)q\,dr, \tag{5}$$

where V denotes the scattering volume. Within the Ornstein-Zernike theory [12] the correlation function of concentration fluctuations is described by

$$G(r)\propto\frac{\exp(-r/\xi)}{r}. \tag{6}$$

A comparison to the static structure factor from the fluctuation theory of Einstein and Smoluchowski [13] leads to a description of the static structure factor

$$S(q)=\langle|\delta c(q)|^2\rangle=k_BTc^2\frac{\chi_T}{1+q^2\xi^2}, \tag{7}$$

where χ_T is the osmotic susceptibility, ξ denotes the correlation length of concentration fluctuations, and k_B is the Boltzmann constant. With respect to Eq. (4), the intensity of scattered light becomes

$$I_s(q)=\frac{C\chi_TT}{1+q^2\xi^2}, \tag{8}$$

where C is a temperature-independent factor containing the macroscopic concentration, the concentration dependence of ε, and k_B. This equation leads to the Ornstein-Zernike-Debye (OZD) method. Since this procedure does not enable us to evaluate the quantity C, we cannot calculate the osmotic susceptibility χ_T itself. Instead we obtain a generalized osmotic susceptibility $C\chi_T$.

Equation (6) is correct only for ranges of r that are not too small. Because of the divergence of the static structure factor in the neighborhood of the critical point, a small number η was introduced by Fisher describing a critical singularity of the correlation function (6). So we can write [14]

$$G(r)\propto\frac{\exp(-r/\xi)}{r^{1-\eta}}. \tag{9}$$

According to renormalization group analysis, one must expect $\eta\approx0.06$ for the three-dimensional (3D) Ising model. Experimental investigations gave values between $\eta=0.065$ [15] and 0.086 [16]. However, for ternary mixtures it is not obvious whether this exponent has to be renormalized in a way like Eq. (1). If we consider the static structure factor exponent, Eq. (8) must be modified to yield

$$I_s(q)=\frac{C\chi_TT}{(1+q^2\xi^2)^{1-\eta/2}}. \tag{10}$$

Because there is no theoretical limit defined for the range of criticality we cannot exclude that corrections to scaling become evident even in the vicinity of the critical point. These corrections modify the power laws, which are determined by a scaling hypothesis. However, approaching the critical point, the amount of these corrections to scaling should decrease and finally disappear.

By application of the renormalization group theory Wegner proposed a description of the critical singularity within an extended range of temperature. For the correlation length he obtained

$$\xi(T)=\xi_0\epsilon^{-\nu}(1+\xi_1\epsilon^{0.5}+\xi_2\epsilon^{1.0}+\xi_3\epsilon^{1.5}),$$
$$\epsilon=\frac{T-T_c}{T_c}. \tag{11}$$

If we disturb a binary critical mixture by adding a third component, we could imagine that in this case the corrections to scaling are applicable even in the critical range. In a binary mixture, however, in the temperature range $T-T_c<1.2\,\mathrm{K}$, the contribution of the Wegner terms $\xi_1,\ldots,\xi_3$ should be close to zero.

B. Scattered light spectrum

Following the theories of Landau and Placzek [17], the linewidth of the central Rayleigh peak in the spectrum of scattered light can be expressed by $\Gamma=D_Tq^2$ in a pure fluid, where D_T is the thermal diffusion coefficient, or by $\Gamma=D_{12}q^2$ in case of a fluid mixture. Here D_{12} denotes the mutual diffusion coefficient. However, this is valid only far from any critical singularity. In the range of criticality we will obtain a strong power-law dependence that can be written as $\Gamma(q)=Aq^z$ with a universal value of the exponent $z=3.066$.

As a result of the mode-mode coupling theory by Kawasaki and Swift [18–20], we identify the linewidth for both singular and regular behavior of a fluid mixture

$$\Gamma=D_{12}q^2\Omega(x)=\frac{Rk_BT}{6\pi\eta\xi}q^2\Omega_0(x)(1+b^2x^2)^{z\eta/2}. \tag{12}$$

In this equation R denotes a dynamic ratio of amplitudes. The scaling variable is defined by $x=q\xi$. The dynamic viscosity is η. The constant $b=0.55$ is an empirical parameter. Equation (12) shows that the dynamic scaling function $\Omega(x)$ can be divided into two parts: (i) the universal Kawasaki function

$$\Omega_0(x)=\frac{3}{4x^2}\left[1+x^2+\left(x^3-\frac{1}{x}\right)\arctan(x)\right] \tag{13}$$

and (ii) a correction term for background viscosity by Bustyn, Sengers, Bhattacharjee, and Ferrell with the critical exponent of viscosity z_η, which is theoretically given by the dynamic scaling law $z=3+z_\eta$.

It is common practice to consider some special cases of Eq. (12).

(i) In the hydrodynamic range, for a very small scaling variable ($q\xi \ll 1$) it follows that

$$\Gamma = Dq^2, \tag{14}$$

where no enlargement of the correlation length is obtained.

(ii) In a cross range with $q\xi \approx 1$, the so-called nonlocal hydrodynamic range, we have to consider a correction for the growth of cooperative regions, so we write

$$\Gamma = D\left(1+\frac{3}{5}q^2\xi^2\right)q^2. \tag{15}$$

(iii) Approaching the critical point ($q\xi \gg 1$) the exponent of q increases to the theoretical value of 3.066. One can obtain a linewith described by

$$\Gamma = D\frac{3\pi}{8\xi^{1+z_\eta}}q^z = \frac{Rk_BT}{16\eta_B Q_0^{z_\eta}}q^z, \tag{16}$$

where η_B denotes the background viscosity, which is a nearly constant regular part of the viscosity, and Q_0 is the critical amplitude of viscosity depending on the system.

C. Viscosity and background correction to linewidth

For a test of dynamic scalings laws as well as for the background correction to the critical linewidth the measurement of viscosity data is necessary. The temperature dependence of viscosity above the plait point is described by

$$\eta = \eta_B(Q_0\xi_0)^{z_\eta}\left(\frac{T-T_c}{T_c}\right)^{-z_\eta\nu}. \tag{17}$$

The noncritical part of viscosity is given by the Vogel equation

$$\eta_B = Ae^{B/(T-C)}, \tag{18}$$

where A, B, and C are temperature-independent constants. They will be determined by viscosity measurements in a temperature range far from critical singularities. With this back-ground viscosity we can calculate the background linewidth of the scattered light according to Rouch and Chen [21].

$$\Gamma_B = 0.038\frac{k_BT}{\eta_B\xi}q^2\frac{1+q^2\xi^2}{Q_0\xi}. \tag{19}$$

This background linewith is used for a correction of the linewidth determined from the time autocorrelation function.

III. EXPERIMENT

A. Sample preparation

1. Glassware cleaning

All light scattering cells, syringes, Erlenmeyer flasks, and viscosimeters were immersed in a mixture of water, sodium hydroxide, and hydrogen peroxide for several days to remove any organic impurities. Then the glassware was rinsed with distilled water and subjected to ultrasonic vibrations for 1 h. Hot water steam was used to remove all remaining dust particles from inside of the flasks and cells. The cleaned glassware was carefully dried at a temperature of 120 °C under vacuum and cooled to room temperature after 8 h under a nitrogen atmosphere. All glassware was sealed with Parafilm before storing.

2. Materials

Certified ACS spectranalyzed cyclohexane (99.5 mole %) and *p*-xylene (99.2 mole %) were used without further purification with the exception of removing traces of water. Both substances were refluxed with calcium hydride and distilled.

The aniline was distilled at 60 °C under reduced pressure using a column 2000 mm in length and dynamically dried with Zeosorb 4A. After repeated rectification the aniline fractions were multiple frozen and evacuated. The substances were stored under an argon atmosphere. A water analysis by Karl-Fischer titration gave less than 12 ppm water in the aniline fractions.

3. Sample preparation

To determine the critical composition coexistence data from Dobbertin [6] (aniline+cyclohexan) and Anglescu and Zinca (aniline+cyclohexane+*p*-xylene) [22] were used. For each plait point we prepared six mixtures with their target compositions. Because of weighing uncertainties, these compositions were slightly different. To avoid the influence of dust the mixtures were filtered through Teflon membranes (with a 0.2 μm pore width) into the cylindrical sample cells. To exclude oxygen and water from the air all operations were carried out under an argon atmosphere. For each system six sample cells were flame sealed to determine the real decomposition temperature $\vartheta_c^{\mathrm{vis}}$. All prepared samples were tested by the volume equivalence criterion. The sample that meets best this criterion was defined to be the critical one. The binary critical mixture was aniline+cyclohexane with 44.58 mole % aniline and a critical decomposition temperature $\vartheta_c^{\mathrm{vis}} = 29.648$ °C. The ternary one was aniline+cyclohexane+*p*-xylene with 44.42 mole % aniline, 49.59 mole % cyclohexane, and $\vartheta_c^{\mathrm{vis}} = 17.576$ °C.

B. Light scattering apparatus

All described light scattering measurements (static and dynamic) are carried out in a commercial apparatus shown in Fig. 1, which is mounted on a vibration-damped table. As the light source we used a NEC-type He-Ne gas laser of about 35 mW at 632.8 nm. Because of the very high scattered light intensity at near critical states the incident beam intensity has been reduced by a liquid crystal attenuator. After passing the attenuator the incident intensity and beam position were ana-

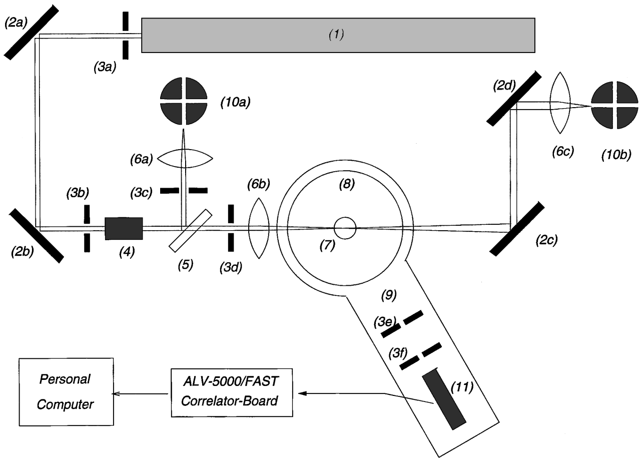

FIG. 1. Light scattering apparatus: (1) He-Ne laser, $(2a)-(2d)$ mirrors, $(3a)-(3d)$ apertures, (4) beam attenuator, (5) beam divider plate, $(6a)-(6c)$ bispherical lenses, (7) probe holder, (8) thermostated measurement cell, (9) goniometer, (10) quadrant photodiodes, and (11) photomultiplier tube.

lyzed using a quadrant-diode coupled in with a beam divider plate. The sample cell was positioned in the center of the scattering cell, which is filled with toluene. To analyze the scattered light a photomultiplier tube was mounted on a goniometer, which allows us to scan a range of angles from 13° up to 152° with an accuracy of better than 0.01°. A fast photon count correlator platine ALV-5000/Fast was connected directly with the photomultiplier and enabled us to obtain lag times down to 13 ns for a dynamic analysis of scattered light.

To determine the quality of optical adjustment, test measurements were carried out with pure toluene as a scattering medium showing no angle dependence of the scattering intensity. During the whole measurement period the angle dependence of scattered light intensity was less than 3%.

We could retain ±0.002 K temperature control over extended periods of time by using a single Julabo-type FP40 thermostat with circulating water as the medium. Temperature measurements in the scattering cell were carried out with a Pt-100 resistor thermometer and a thermistor that has a sensitivity of better than 0.2 mK.

C. Scattered light measurement

After centrifugation to avoid dust particles in the scattering volume, the sample cell was positioned into the apparatus. It was allowed to come to thermal equilibrium by observing the scattered intensity over a time range of about 2–3 h.

Both static and dynamic measurements of scattered light were done simultaneously at the same apparatus. In both binary and ternary samples we measured intensities at 21 angles between 40° and 140° and 117 temperatures in a range from $T-T_c=0.02$ to 1.2 K. The sampling time at each angle and temperature was 10 s. This procedure was repeated ten times to get 100 s of total measurement time interrupted by 5 s of the autoscaling procedure between each sampling period.

The measured scattering intensity I_s was corrected for scattering volume, intensity fluctuations, dark counts, etc., according to the methods proposed by Kao and Chu [23]. To extract the effect of criticality from our measurements we applied the following procedure for background correction. We used the same mixture and measured the intensity of scattered light at 35 K above the critical temperature. At this high temperature no critical effects are expected and this I_B is taken for the background correction. The corrected intensity is denoted by I_{sc}.

D. Viscosimetry

The behavior of a near critical mixture is very sensitive to slight changes in its composition. Since a common Ubbelohde viscosimeter is an open system, we did not obtain reliable measurements. Instead we modified the viscosimeter so that it could be flame sealed. To move the substance in the upper part of the viscosimeter it was mounted on a plate that enables a vertical rotation. This apparatus was placed in a water bath with a volume of about 45 l. By using a Julabo-type thermostat FP25 we achieved a constant temperature with fluctuations less than ±0.005 K over a time range of 24 h. The rotating plate was driven by an external motor in order to avoid any influence on the bath temperature.

The related density needed to calculate the dynamic viscosity from flow times was measured with a vibration densimeter (Fa. A. Paar), which uses the density-dependent damping of a U-shaped vibrating tube containing the sample. This apparatus must be calibrated by well known density standards. We used the pure substances of aniline and cyclohexane as standards. A temperature constant of about ±0.002 K was achieved with the help of another Julabo-type thermostat FP40.

IV. DATA ANALYSIS

Since the temperature dependence of the observed properties in the critical range is strongly nonlinear, the application of a special powerful least-squares fitting procedure became essential. Instead of a standard implementation of the Marquard-Levenberg algorithm we applied a special procedure of Golub and Pereyra [24] and Osborne [25]. They designed an algorithm to solve problems of a type of multiple nonlinear regression with a model function Y_{calc} that is separable. The program attempts to compute a weighted least-squares fit to a separable function

$$Y_{\mathrm{calc}}(\alpha,\beta,x)=\sum_{j=1}^{L}\beta_j\Phi_j(\alpha,x)+\Phi_{j+1}(\alpha,x), \qquad (20)$$

which is a linear combination of nonlinear functions Φ_j. It determines L linear parameters β_j and the vector of nonlinear parameters α by minimizing the norm of residuals r

$$|r|^2=\sum_{i=1}^{N}W_i[Y_i-Y_{\mathrm{calc}}(\alpha,\beta,x_i)]^2, \qquad (21)$$

where W_i denotes the weight of each point (Y_i,x_i). This weight is given by the reciprocal of the square of the uncertainty for that measured point. The residual r is modified to incorporate, for any fixed α, the optimal linear parameters for that α. It is then possible to minimize only the nonlinear

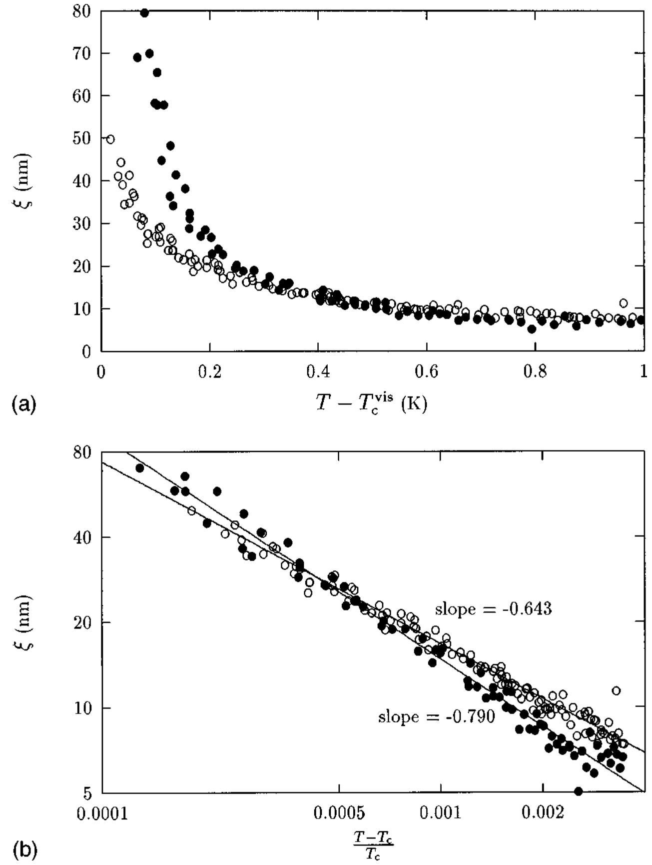

FIG. 2. Correlation length of the critical concentration fluctuations ξ vs temperature of the binary (○) and ternary (●) mixture. (a) Correlation length ξ vs $T-T_c^{\mathrm{vis}}$, where T_c^{vis} is the visually obtained critical temperature. (b) A log-log plot of the correlation lengths vs the reduced temperature. This corresponds to the power law approximation.

parameters. After the optimal values of the α have been determined, the linear parameters can be recovered by linear least-squares techniques [24]. This is achieved by a modification (see [25]) of the Marquard-Levenberg procedure using stable orthogonal Householder reflections on a modification of the Jacobian.

The main advantage of this procedure over other least-squares programs is that no initial guesses are needed for the linear parameters. Not only does this make it easier to use, but it often leads to faster convergence. We used this program code VARPRO for the determination of the critical amplitudes, exponents, and critical temperatures as well as for the calculation of the Wegner coefficients. Here we especially benefited from the fact that the objective function Y is separable. We treated the critical exponent as a nonlinear parameter and the Wegner coefficients as linear parameters.

V. RESULTS AND DISCUSSION

A. Static properties

1. Determination of correlation lengths and osmotic susceptibilities

According to Eq. (7), we used the common procedure by Ornstein, Zernike, and Debye

$$\frac{I_B T}{I_{\mathrm{sc}}(q)} = \frac{1}{C\chi_T} + \frac{\xi^2}{C\chi_T} q^2 \tag{22}$$

to determine the generalized osmotic susceptibility and the correlation length from the corrected scattering intensity at a given temperature. Using this method we calculated the susceptibility $C\chi_T(T)$ from the scattered intensity at zero angle and the correlation length $\xi(T)$ from the slope. The correlation lengths of the binary and the ternary critical mixture, as calculated according to Eq. (22) vs temperature are shown in Fig. 2. We were not able to give a single estimate for the uncertainities $\Delta\xi$ of $\xi(T)$ over the whole range of measured temperatures. However, we can specify estimates for following cases: (i) In the range $T-T_c \gg 1.5\,\mathrm{K}$, due to the low scattering intensity, we found $\Delta\xi \approx 5\,\mathrm{nm}$; (ii) if $T-T_c = 1.5-0.2\,\mathrm{K}$ the higher intensity leads to $\Delta\xi < 1\,\mathrm{nm}$; and (iii) at $T-T_c < 0.2\,\mathrm{K}$ the system became very sensitive to temperature fluctuations and the uncertainities increase to $\Delta\xi \approx 10\,\mathrm{nm}$. If we compare our results for the binary and ternary mixtures [see Fig. 2(a)] we find only slight differences in the range far from the critical temperature. If $T-T_c$ becomes less than 0.4 K, the difference in both correlation lengths becomes evident and leads to an apparently stronger curvature of the ternary correlation length. To eliminate the temperature effect on this curvature a log-log plot of the correlation length versus the reduced temperature was made [Fig. 2(b)].

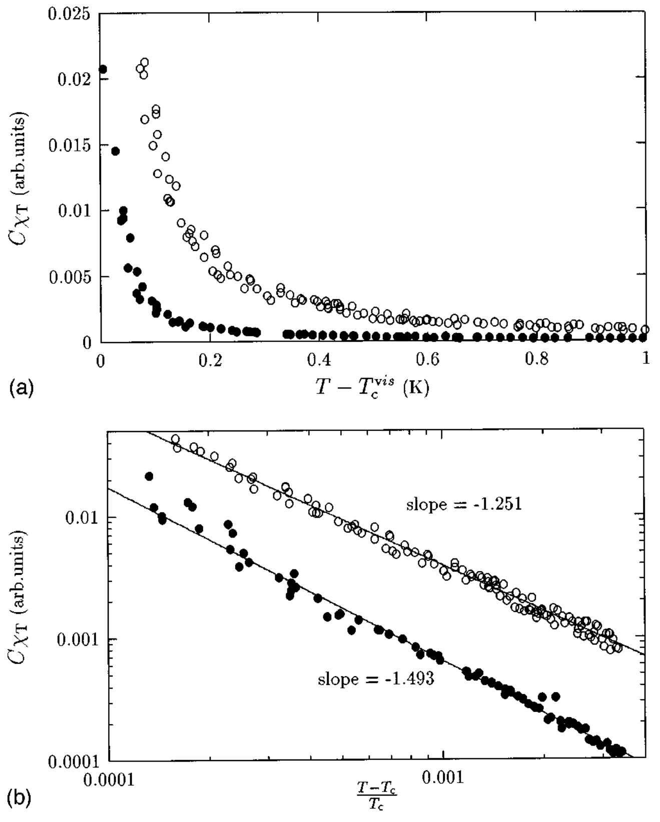

FIG. 3. Temperature dependence of the generalized osmotic susceptibility $C\chi_T$ for a binary (○) and ternary (●) mixture. (a) $C\chi_T$ vs $T-T_c^{\mathrm{vis}}$, where T_c^{vis} is the visually obtained critical temperature. (b) A log-log plot of the susceptibility vs the reduced temperature. The slopes give the values of the critical exponents.

TABLE I. Results of fitting the temperature dependence of correlations lengths of the binary system $\xi(T)$ to a simple power law and to scaling corrections.

Parameter	According to Eq. (23)		According to Eq. (26)		According to Eq. (25)	
ξ_0	0.223	±0.016	0.212	±0.018	0.121	±0.015
ξ_1			0.023	±0.008	62.64	±69.73
ξ_2					−2710.74	±31003
ξ_3					11438.02	±12759
T_c	302.765	±0.003	302.768	±0.004	302.781	±0.004
ν	0.633	±0.011	0.641	±0.012	0.728	±0.126
variance	1.777		1.676		1.683	

From the zero angle limit of Eq. (22) we obtain the generalized osmotic susceptibility $C\chi_T$, the temperature dependence of which is presented in Fig. 3(a). Again the curvature of the ternary mixture data is stronger than that of the binary mixture. Figure 3(b) shows that in the ternary case a nonlinearity was found at temperatures lower than 0.1 K above the critical point. Two effects have to be considered in this case: (i) The influence of multiple scattering leads to higher intensities and thus to higher values of the susceptibility and (ii) the correction for background scattering depends on the precision of incident beam measurements. At low incident intensities, because of the very intense scattering, we reach the limit of incident intensity resolution. To avoid errors resulting from this nonlinearity, we used only the linear part of the data set to obtain the critical susceptibility exponents γ and γ_x.

2. Calculation of the static critical exponents by power laws

Our data were measured very close to T_c. Therefore, we assume that power laws will describe the temperature dependence of the correlation length

$$\xi(T)=\xi_0\left(\frac{T-T_c}{T_c}\right)^{-\nu} \tag{23}$$

and generalized osmotic susceptibility

$$C\chi_T(T)=C\chi_{T,0}\left(\frac{T-T_c}{T_c}\right)^{-\gamma}. \tag{24}$$

To determine the parameters in Eqs. (23) and (24) we performed nonlinear least-squares fits applying the VARPRO code described above. As input we used weighted $\xi(T)$ and C_{χ_T} data from the OZD method. The critical amplitude was considered as a linear parameter, whereas T_c and the exponents were treated as nonlinear parameters in the fit. As shown in the first two columns of Table I–IV, we achieved satifying fits with reasonable results for both properties. Within their uncertainties the critical exponents for the binary mixture show the expected values of the 3D Ising model. In the ternary mixture the exponents of correlation length and osmotic susceptibility are apparently larger. Simultaneously in the ternary mixture, the critical amplitudes of both variables became much smaller than in the binary ones. This is a numerical effect due to the strong coupling between the critical exponent and the corresponding amplitude in the power laws.

3. Determination of the static exponents by correction to scaling

There is conjecture that the presence of a third component in a critical mixture may not only alter the critical exponent but also influence the correction to scaling. To investigate this behavior in more detail we applied a Wegner expansion to our correlation length data $\xi(T)$ and determined the critical exponent ν. The Wegner expansion (11) was rearranged

$$\xi(T)=\xi_0\epsilon^{-\nu}+\xi_0\xi_1\epsilon^{0.5-\nu}+\xi_0\xi_2\epsilon^{1.0-\nu}+\xi_0\xi_3\epsilon^{1.5-\nu} \tag{25}$$

to suit a nonlinear regression with separable terms, where the amplitude ξ_0 and the Wegner coefficients appear as linear parameters and T_c and ν as nonlinear ones. The experimental data were weighted by their respective reciprocal square variances obtained from the slope of the OZD method. To study the influence of the third component we applied the same fitting procedure to the data of the binary mixture too.

TABLE II. Results of fitting the temperature dependence of correlations lengths of the ternary system $\xi(T)$ to a simple power law and to scaling corrections.

Parameter	According to Eq. (23)		According to Eq. (26)		According to Eq. (25)	
ξ_0	0.052	±0.012	0.091	±0.011	−0.012	±0.003
ξ_1			0.087	±0.017	−553.33	±509.38
ξ_2					15083.33	±14843
ξ_3					−135250.32	±154343
T_c	290.771	±0.007	290.773	±0.007	290.822	±0.005
ν	0.820	±0.037	0.743	±0.020	0.758	±0.116
variance	2.225		2.209		2.205	

TABLE III. Results of fitting the temperature dependence of the osmotic susceptibility $C\chi_T(T)$ of the binary mixture to a simple power law and to scaling corrections.

Parameter	According to Eq. (24)		According to Eq. (28)		According to Eq. (27)	
χ_{T0}	1.811	±0.210	1.852	±0.188	1.89	±0.19
χ_{T1}			0.062	±0.021	7.16	±6.75
χ_{T2}					−221	±223
χ_{T3}					493	±452
T_c	302.768	±0.004	302.752	±0.006	302.742	±0.018
γ	1.253	±0.028	1.252	±0.022	1.244	±0.107
variance	4.285		4.274		4.171	

In a first step we performed a four-parameter fit, treating ξ_0 and the ξ_1 as linear parameters and T_c and ν as nonlinear ones. The higher coefficients were set to zero

$$\xi(T)=\xi_0\epsilon^{-\nu}+\xi_0\xi_1\epsilon^{0.5-\nu}. \tag{26}$$

For both the binary and ternary mixtures the results of this procedure are shown in the third and fourth columns of Tables I and II. In both cases correction to scaling leads to small improvements of the fit shown by a decrease in variance. In the case of our binary mixture, the introduction of the second term in Eq. (26) leads only to slight changes in the values of critical exponent and amplitude. Consequently, this first correction term is small. In the ternary mixture, however, the results show a considerable downward change of the critical exponent if we apply a Wegner term as in Eq. (26). Here the value of this term becomes more significant and should not be left out. The critical temperatures determined by using Eq. (26) are within the uncertainities of our direct measured decomposition temperatures. Fixing the critical exponents to their theoretical values does not lead to significant changes in the values of the free parameters or in the quality of the fit.

To test the influence of the higher-order terms we used Eq. (25) performing a six-parameter fit, treating ξ_0 and the ξ_i as linear parameters and T_c and ν as nonlinear ones. For the binary system we found good agreement in T_c and a critical exponent ν that is larger than that from the simple power law (23). However, it has a statistical uncertainity considerably larger than the former. For the ternary system the estimated critical temperature increases about 50 mK, which is outside our direct measurements of the decomposition temperature. The ternary critical exponent decreases to a value of $\nu_x=0.76$. However, the critical amplitude of the ternary mixture exhibits an unphysical value that leads to a downward singularity of the first term in Eq. (25). This behavior compelled us to analyze the various terms in the corrections to scaling under the assumption that approaching the critical temperature these corrections should tend to zero.

In a first run the critical exponent was kept fixed at $\nu_x=0.71$. We found a slight decrease in the variance and results as shown in Fig. 4. In this diagram we see that the power-law term improves at the expense of the first Wegner term. The overall result (solid line) is in good agreement with the experimental data, but the various Wegner terms differ widely. They describe closely the critical singularity itself, but not any corrections to scaling. The first and second correction terms are rather large, have opposite signs, and seems to compensate for each other, whereas the third term tends towards zero at T_c, as expected. The next diagram (Fig. 5) represents the fitting results when we use the value of the critical exponent $\nu_x=0.63$, as predicted for the 3D Ising model. The quality of the representation still improved. The power-law term shows even closer agreement with the measured correlation lengths and the Wegner terms nearly compensate for each other.

To find out whether this procedure converges we determined the run with the minimum overall variance. The corresponding critical exponent is $\nu_x=0.50$ and the detailed representation is given in Fig. 6. Here the power-law term is close to the experimental data and gives a good description of the critical region. The Wegner expansion terms tends towards zero as we expected and are influenced more if the distance from T_c increases. However, in all cases we should keep in mind that the differences in variance are quite small and the statistical uncertainities are rather high.

TABLE IV. Results of fitting the temperature dependence of the osmotic susceptibility $C\chi_T(T)$ of the ternary system to a simple power law and to scaling corrections.

Parameter	According to Eq. (24)		According to Eq. (28)		According to Eq. (27)	
χ_{T0}	0.408	±0.041	0.373	±0.03	0.071	±0.014
χ_{T1}			0.113	±0.02	339.71	±293.54
χ_{T2}					−575	±561
χ_{T3}					16042	±16436
T_c	290.778	±0.010	290.772	±0.009	290.751	±0.009
γ	1.542	±0.047	1.422	±0.051	1.471	±0.102
variance	4.812		4.732		4.799	

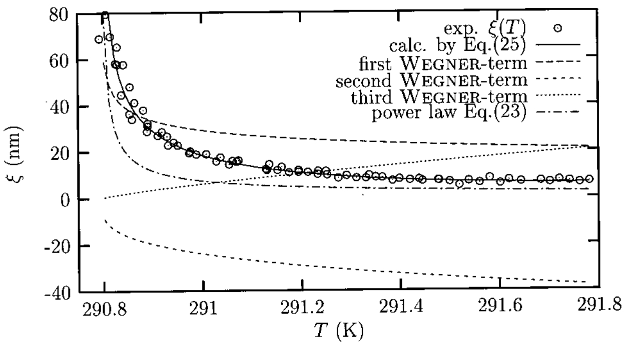

FIG. 4. Wegner expansion of the correlation length $\xi(T)$ for the ternary mixture with a critical exponent $\nu_x = 0.71$. Comparison of experimental data (○) with the full correction to scaling [Eq. (25)], the first (power law) term [Eq. (23)], and the individual Wegner terms.

From this detailed analysis we conclude that for our experimental data a Wegner expansion does not yield significant improvement. We feel that in our case the expansion with $\nu_x = 0.50$ gives the best and physically most reasonable representation, but generally it seems preferable to restrict ourself to a power-law analysis with only one Wegner term. Our results illustrate the difficulties in the determination of a critical exponent because the superposition of the Wegner correction terms tends to a certain self-compensation.

A similar analysis was performed for the generalized osmotic susceptibilities $C_{\chi_T}(T)$. We intended to calculate the critical exponent γ_x from a Wegner expansion with separated correction to scaling terms:

$$C\chi_T(T) = \chi_0\epsilon^{-\gamma} + \chi_0\chi_1\epsilon^{0.5-\gamma} + \chi_0\chi_2\epsilon^{1.0-\gamma} + \chi_0\chi_3\epsilon^{1.5-\gamma}. \tag{27}$$

Again we found a slight improvement of the representation when we included the correction to scaling. As shown in Tables III and IV, the values of the critical exponents γ and γ_x for the binary and ternary mixtures decrease. The ternary system shows a susceptibility exponent larger than the binary one. As in the case of the correlation length, we varied the critical exponent and determined the expansion coefficients. The minimum overall variance was reached at $\gamma_x = 1.20$, but the Wegner coefficients had large statistical uncertainities.

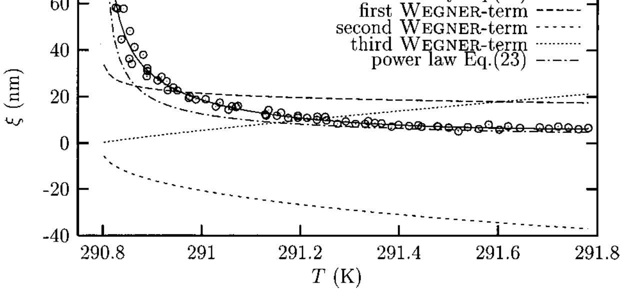

FIG. 5. Wegner expansion of the correlation length $\xi(T)$ for the ternary mixture with a critical exponent $\nu_x = 0.63$. The parameters are the same as in Fig. 4.

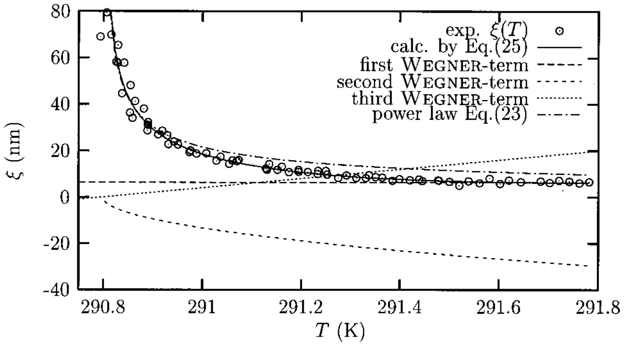

FIG. 6. Wegner expansion of the correlation length $\xi(T)$ for the ternary mixture with a critical exponent $\nu_x = 0.50$. The parameters are the same as in Fig. 4.

Similar to the case of the correlation lengths, the best analysis was obtained by restriction to one correction term

$$C\chi_T(T) = \chi_0\epsilon^{-\gamma} + \chi_0\chi_1\epsilon^{0.5-\gamma} \tag{28}$$

even if the variance of the fit is slightly larger than that from Eq. (27). In the case of the binary mixture the additional parameter does not change significantly both the critical exponent and the critical temperature determined by simple power laws. The small value of the correction term is in agreement with this result. The exponent shows nearly its theoretical value. If we investigate the ternary mixture the first-order scaling correction according to Eq. (28) becomes significant. Consequently, the determined critical exponent tends to decrease. Unlike the higher-order Wegner expansion (27), in the present case all parameters were obtained with sufficient precision.

4. Influence of the structure factor exponent

Equation (22) does not consider the singularity η of the static structure factor $S(q)$. To test the influence of η the least-squares fitting procedure was used to determine the values of the critical exponents ν, γ, and η (ν_x, γ_x, and η_x for ternary mixture) and the critical amplitude ξ_0 (ξ_{0x}) by a modified Fisher equation [14]

$$\frac{I_{\mathrm{sc}}}{T} = A_0\epsilon^{-\gamma}[1+q^2\xi_0^2\epsilon^{-2\nu}]^{-1+\eta/2} + I_B, \tag{29}$$

where ϵ denotes the reduced temperature $(T-T_c)/T_c$, A_0 is treated as a parameter, and I_B is the background scattering intensity. Because of the background correction included in I_{sc}, I_B was zero. In both binary and ternary critical mixtures we could not find a significant difference between the results of the five-parameter fit (A_0, γ, ν, η, and ξ_0) and the OZD method with a three-parameter fit to a power law either in the binary or in the ternary mixture. The slight difference in the exponents ν and γ calculated with Eq. (29) (see Table V) is within the range of uncertainity. It is interesting that we found a structure factor exponent η_x for ternary mixtures comparable to the binary one. This does not lead to a renormalization of η. However, the structure factor exponent is very small; it is within the uncertainties of the other exponents. We have summarized the results of both methods for the binary mixture in Table V and for the ternary system in Table VI.

TABLE V. Summary of the critical exponents of the binary mixture resulting from data analysis using the OZD method (22) and the modified Fisher equation (29).

Equations \ Exponents	ν	γ	η
(22)–(24)	0.643±0.024	1.251±0.056	
(29)	0.636±0.031	1.244±0.042	0.045±0.011

B. Transport properties

1. Determination of the mutual diffusion coefficient

At the same angles and temperatures at which we measured the scattered intensity, we obtained the time-autocorrelation function

$$G^{(2)}(\tau)=\frac{1}{N}\sum_{k=1}^{N} I(k)I(k+\tau),$$

$$k=1,...,N \text{ correlator channels,} \tag{30}$$

of the intensity by a multiple-τ hardware correlator. After a symmetric normalization

$$g_s^{(2)}=\frac{MG^{(2)}(k)-M_0M_k}{M_0M_k}, \tag{31}$$

with $M_0=\Sigma_{k=1}^{N}I(k)$ and $M_k=\Sigma_{k=1}^{N}I(k-1)$, we applied the Discrete algorithm by Provencher [26] to calculate the linewidth Γ of each signal. Because of the relaxation processes in both binary and ternary mixtures one can obtain only one relaxation time. To determine the mutual diffusion coefficient for each temperature a linear plot of $\Gamma(q)/q^2$ vs q^2 was performed. We identify the zero-angle linewidth

$$D_{12}=\lim_{q\to 0}\left(\frac{\Gamma_c}{q^2}\right)_T \tag{32}$$

as the mutual diffusion coefficient. The term Γ_c denotes the critical part of the scattered linewidth calculated by $\Gamma_c=\Gamma-\Gamma_B$, where Γ_B is the background linewidth according to Eq. (19). Here it was not necessary to measure the absolute scattering intensity, so the diffusion coefficients are the most precise properties we obtained within this work. The variances are less than 1% within a range of $T-T_c>0.1\,\text{K}$. Figure 7 shows the temperature dependence of the measured diffusion coefficients in the binary and the ternary mixtures. One can see the critical slowing down of the mutual diffusion. Both the binary and ternary mixtures show almost no diffusion at the critical temperature. However, our ternary system exhibits a less strong curvature and a much lower diffusion coefficient in the hydrodynamic range. This is remarkable because of the only small difference between the correlation lengths in the binary and the ternary mixture. The log-log plot of the mutual diffusion coefficients vs the reduced temperature [lower part of Fig. 7(b)] reveals the influence of the different critical exponents of the diffusion coefficient in both mixtures, as one can see from the slopes. Especially for the correct calculation of the viscosity exponent, it is important to know the temperature range of criticality in the binary and ternary mixtures. There is no exact theoretical criterion to tell us in which temperature range the applied power laws are valid. However, the value of the linewidth exponent z describing the q dependence of the linewidth is a suitable practical criterion for this purpose. We obtain the effective linewidth exponent z_{eff} by estimation of $\Gamma=D_{12}q^{z_{\text{eff}}}$. Figure 8 shows the growth of z_{eff} vs the temperature difference $T-T_c$. We find an enlargement of the linewidth exponent from $z_{\text{eff}}\approx 2$ (hydrodynamic range) to higher values in order to reach the critical temperature in both cases. The ternary mixture shows a smaller critical range.

TABLE VI. Summary of the critical exponents of the ternary mixture resulting from data analysis using the OZD method (22) and the modified Fisher equation (29).

Equations \ Exponents	ν_x	γ_x	η_x
(22)–(24)	0.790±0.033	1.493±0.070	
(29)	0.784±0.041	1.490±0.068	0.058±0.016

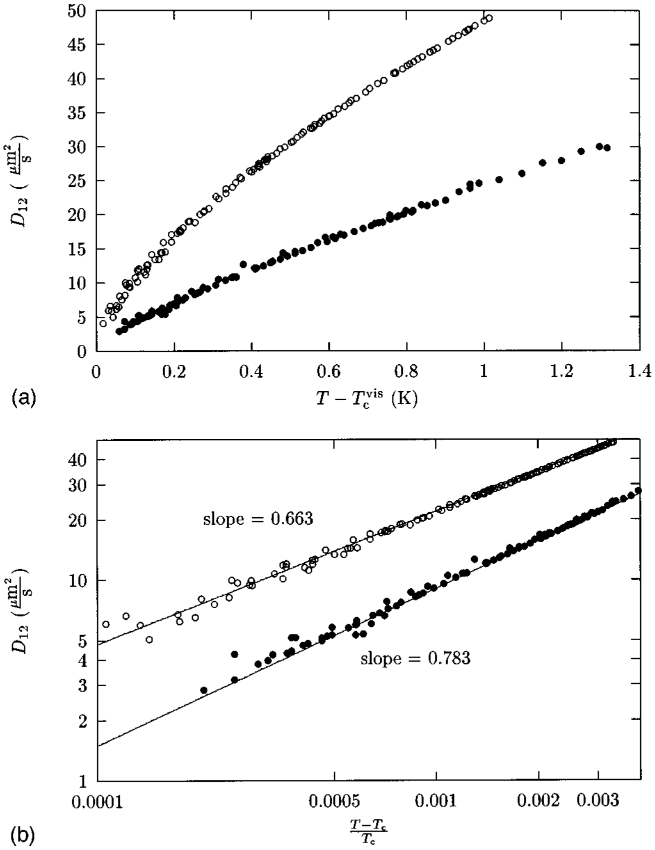

FIG. 7. Temperature dependence of the mutual diffusion coefficients D_{12} for a binary (○) and ternary (●) mixture. (a) D_{12} vs $T-T_c^{\text{vis}}$, where T_c^{vis} is the visually obtained critical temperature. (b) A log-log plot of the mutual diffusion coefficients vs the reduced temperature. The straight lines show the approximation to power laws.

2. Calculation of the critical diffusion exponent by power laws

Since our measurements were performed very close to T_c, we assumed that the temperature dependence of the mutual diffusion coefficient can be described by a simple power law

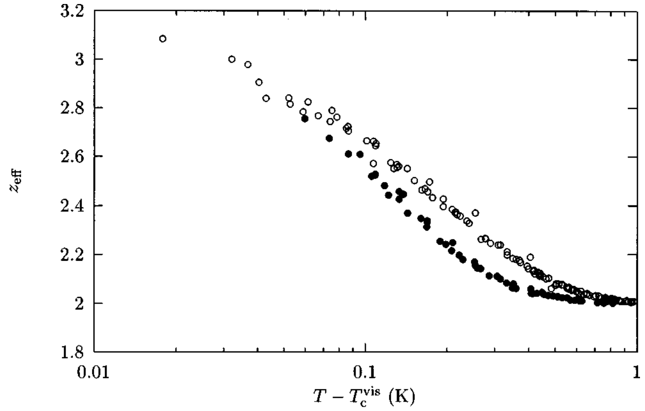

FIG. 8. Plot of the effective linewidth exponent z_{eff} vs the temperature above the critical point for the binary (○) and ternary (●) mixture.

$$D_{12}=D_{12,0}\left(\frac{T-T_c}{T_c}\right)^{\nu^*}. \tag{33}$$

Like our static data analysis, we used the VARPRO nonlinear least-squares algorithm to perform a free fit of our binary and ternary data to this model. The results of this calculation are shown in Tables VII and VIII. Within the statistical uncertainties the determined critical temperature agrees with the values of T_c found from the analysis of the static properties by power laws. The critical exponent of the binary diffusion coefficient shows a slightly smaller value than the theoretical one from the dynamic renormalization theory ($\nu^*_{\mathrm{theor}}=0.67$). The critical diffusion exponent of the ternary mixture ν^*_x is apparently larger. This is consistent with an increased exponent of the correlation length in the ternary case. Again one can see the strong coupling between the critical exponent and the critical amplitude $D_{12,0}$, which leads to a smaller value of the amplitude in the case of the ternary mixture.

3. Determination of the diffusion exponent by correction to scaling

The mutual diffusion coefficient is strongly connected to the hydrodynamic radius of the moving particles. If we assume that the third component influences the corrections to scaling of the correlation length, we have to investigate the same assumption in the case of diffusion coefficients too. Therefore, we tried to calculate the exponent ν^* of $D_{12}(T)$ taking into consideration the scaling corrections

$$D_{12}(T)=D_{12,0}\epsilon^{-\nu^*}+D_{12,0}D_{12,1}\epsilon^{0.5-\nu^*}+D_{12,0}D_{12,2}\epsilon^{1.0-\nu^*}+D_{12,0}D_{12,1}\epsilon^{1.5-\nu^*}. \tag{34}$$

The results of this data analysis are shown in Tables VII and VIII. Similar to the behavior of the static properties, we found a small decrease of the variance if we included corrections to scaling according to Eq. (34). While in the case of static properties we observed larger changes in the calculated temperatures, for the diffusion coefficients these differences are within the uncertainties. The accuracy of the calculated critical exponents is comparable to that of the results obtained from power-law fitting. We found only small differences between exponents calculated from a power law and those from scaling corrections. Again the exponent of the ternary system is larger than the binary one. Also in the case of the mutual diffusion coefficient an exact calculation of Wegner coefficients was not possible because of the large uncertainties. The relatively small changes in all parameters lead to the assumption that the model (27) might be overestimated.

To avoid this overestimation we restrict the scaling correction even more to one Wegner term

$$D_{12}(T)=D_{12,0}\epsilon^{-\nu^*}+D_{12,0}D_{12,1}\epsilon^{0.5-\nu^*}. \tag{35}$$

Compared to the fit from simple power laws, we yield downward changes of the critical exponents in both the binary and the ternary system. Consequently, the first Wegner terms are of the same order. This leads to the assumption that the diffusion coefficient is influenced by the noncritical part of the dynamic viscosity in the binary system. Unlike the full scaling corrections, the results of this fit are more satisfying because of the smaller uncertainties in the determination of the parameters.

C. Dynamic viscosity

To determine the scaling behavior we measured the flow times of the mixtures at 104 temperatures in the range from 20 mK up to 2 K above the critical temperature. To avoid the influence of background viscosity we also performed measurements from $T-T_c=4$ K ($z_{\mathrm{eff}}\approx 2$) up to $T-T_c=30$ K and used these data to estimate the parameters of the Vogel equation (18), as shown in Table IX. The temperature-

TABLE VII. Results of fitting the temperature dependence of the mutual diffusion coefficient $D_{12}(T)$ of the binary system to a simple power law and to scaling corrections.

Parameter	According to Eq. (33)		According to Eq. (35)		According to Eq. (34)	
$D_{12,0}$	2747	±78	2733	±81	1976	±61
$D_{12,1}$			0.042	±0.001	0.0022	±0.0015
$D_{12,2}$					−0.0312	±0.0204
$D_{12,3}$					0.0644	±0.0656
T_c	302.763	±0.003	302.771	±0.006	302.788	±0.01
ν^*	0.657	±0.012	0.638	±0.011	0.643	±0.016
variance	2.173		2.148		2.151	

TABLE VIII. Results of fitting the temperature dependence of the mutual diffusion coefficient $D_{12}(T)$ of the ternary system to a simple power law and to scaling corrections.

Parameter	According to Eq. (33)		According to Eq. (35)		According to Eq. (34)	
$D_{12,0}$	1048	±46	1087	±111	1117	±51
$D_{12,1}$			0.062	±0.013	0.010	±0.008
$D_{12,2}$					−0.0699	±0.0518
$D_{12,3}$					0.1940	±0.2003
T_c	290.775	±0.005	290.778	±0.006	290.782	±0.008
ν^*	0.787	±0.021	0.751	±0.046	0.781	±0.14
variance	3.025		2.975		2.982	

dependent flow times from viscosity measurements were corrected by the Hagenbeck formula. We obtained the dynamic viscosities by

$$\eta(T)+\eta_B(T)=K[t(T)-t_h]\rho(T) \tag{36}$$

using temperature-dependent densities from the vibration densimeter. The viscosities for the binary and ternary mixtures vs the temperature are shown in Fig. 9. For the ternary mixture the absolute values of the dynamic viscosity are apparently higher. This is in agreement with the lower diffusion coefficient at similar correlation lengths in this mixture. However, we did not observe a significant difference in the curvature of both viscosities vs temperature. Taking experimental uncertainties into account, the log-log plot, as shown in Fig. 9(b), does not yield different slopes. In this connection we note that the use of a vibration densimeter for measurements in the critical range should be considered with care. The system is very sensitive to the import of mechanical energy that may shift the system away from the near critical state. The application of a capillary viscosimeter leads to shear forces during the measurement that disturb the laminar flow process. Because of this our results of the viscosity measurements are the most uncertain ones. To determine the viscosity exponent z_η we used Eq. (17) with the values of ξ_0 and ν from our static light scattering measurements. Like the structure factor exponent, z_η is very small. Because of this situation we did not perform an analysis of possible scaling corrections. In addition, this should be unnecessary because of the viscosity background correction by Vogel.

VI. SUMMARY

The purpose of this investigation was to study critical singularities in binary and ternary fluid mixtures, in particular the determination of critical exponents in these systems. Since we performed the same experimental and fitting procedures on both mixtures under the same conditions, we can directly compare the behavior of these systems and determine changes in their critical properties. We investigated the shift in critical exponents, the validity of power laws, the influence of the structure factor exponent, and the role of corrections to scaling when we change from a binary critical mixture to a ternary one. There is a significant difference between a binary critical point and a ternary plait point. The plait point is part of a critical line on a coexistence surface. Therefore, any thermodynamic path approaching the ternary plait point may or may not come close to this critical line. Thus its shortest distance to the critical line may vary [27]. Our basic assumption is that this behavior will influence the critical properties. Instead of a single value, this would lead to a sequence of critical exponents, depending on the shortest

TABLE IX. Critical exponent z_η according to Eq. (17) and the parameters of Eq. (18) by Vogel describing the noncritical part of the dynamic viscosity.

System	z_η	A (cP)	B (K)	C (K)
binary	0.045±0.021	0.1032	201.358	204.771
ternary	0.054±0.028	0.1019	184.359	193.146

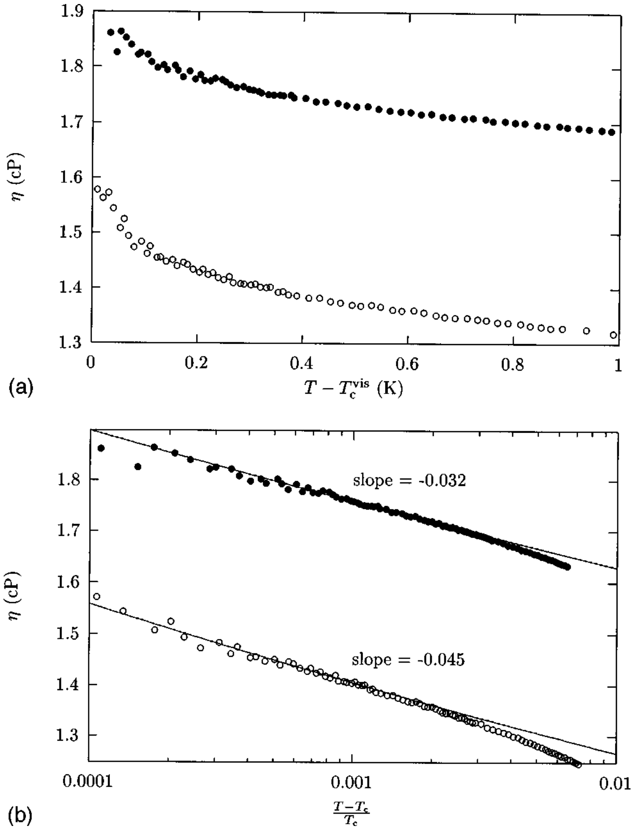

FIG. 9. Temperature dependence of the critical part of the dynamic viscosity η for the binary (○) and ternary (●) system. (a) η vs $T-T_c^{\text{vis}}$. (b) Dynamic viscosity vs the reduced temperature. The slopes of the straight lines correspond to the critical exponents.

distance to the critical line. The binary exponent should be the limit of this sequence. To study these assumptions we found that more high-precision experimental data on ternary systems are needed and especially data sets over a wider range of temperatures so that the role of scaling corrections could be investigated in more detail.

First we applied simple power laws to describe the temperature dependence of our experimental data and we obtained good agreement between the calculated critical temperature and the measured decomposition temperature of the same mixture. In the binary mixture case the critical exponents ν, γ, and ν^* show only small differences from the theoretical values. When we applied the power laws to the ternary mixture data we found critical exponents ν_x, γ_x, and ν_x^* that are apparently larger than the binary ones.

There is a conjecture that adding a third component to a binary critical mixture may not only alter the critical exponent but also change or influence the corrections to scaling. This behavior might be interpreted by the hypothesis of shortest distance to the critical line. On a thermodynamic path to a critical plait point the shortest distance to the critical line may change, depending on whether the path is close to or distant from the critical line. This change in distance to the critical state could lead to a change in the corrections to scaling. Therefore, we used the static properties correlation length and generalized osmotic susceptibility to investigate this influence. Generally, the introduction of scaling corrections leads to a downward shift of the critical exponents.

From our data analysis we found that the application of several correction terms does not lead to consistent, physically meaningful results. Because of the superposition of additional terms, the correction tends to self-compensation. The resulting values of such correction terms become meaningless. Therefore, it is important to choose the order of correction to scaling carefully, that is, in our case only one Wegner term. We observed that the effect of the third component is represented in two parameters: an enlargement of the critical exponent and a nonzero first-order correction term. The first follows from the renormalization explained by the mobile electron Ising model. We found no significant difference from the results of this model if we applied the first-order correction. We can conclude that the ternary aniline+cyclohexane+p-xylene system shows no simple Ising-like behavior in the range of critical singularity. The first-order correction term is necessary to describe the temperature dependence of the measured static properties in ternary systems. Because of the limitation of the 3D Ising model to only two possible states on each lattice site this result should be expected.

An exception was found with the viscosity measurements. The comparison with the theoretical binary exponent shows that our measured values are too low. Unlike the other data sets, we could not obtain any significant difference between the viscosity exponent z_η in the binary and $z_{\eta,x}$ in the ternary mixture with respect to their uncertainties.

It would be interesting to test the estimated critical exponents to static scaling laws. If the observed systems are members of an universality class, the equations

$$(2-\eta)\nu=\gamma, \quad (2-\eta)\nu_x=\gamma_x \tag{37}$$

should hold for binary and ternary systems, respectively. For the experimental exponents of the binary mixture this law holds, as expected. In the ternary case we found a difference between the right- and left-hand sides of Eqs. (37). However, this difference is smaller than the deviation of the exponents ν_x and γ_x. Therefore, we assume that this scaling law holds for ternary systems too.

The connection between static and dynamic critical exponents is given by the scaling laws

$$\nu^*=\nu(1+z_\eta), \quad \nu_x^*=\nu_x(1+z_{\eta,x}), \tag{38}$$

respectively. Since the exponent ν_x^* of mutual diffusion is smaller than the correlation length exponent ν_x, this scaling law does not hold for our ternary mixture.

There is no doubt of the universality in ternary mixtures in the vicinity of their critical points with respect of their static properties. The enlargement of the measured static exponents does not lead to a violation of the static scaling law. However, for dynamic properties we did not find the same behavior.

The results of our measurements show that the addition of a third component to a binary critical system along a critical line leads to an enlargement of the static and dynamic critical exponents. Further investigations at various points along the critical line will show whether these values are fixed or functions of the binodal surface slope.

ACKNOWLEDGMENTS

We gratefully acknowledge financial support of this research by the Deutsche Forschungsgemeinschaft (Grant No. AZ Wi 1081/8-1). We wish to thank the Department of Physical Chemistry of the University of Cologne for technical support.

[1] B. Berne and R. Pecora, *Dynamic Light Scattering* (Plenum, New York, 1985).
[2] B. Chu, *Laser Light Scattering* (Academic, London, 1982).
[3] B. Volochine, Ber. Bunsenges. Phys. Chem. **76**, 217 (1972).
[4] P. Berge and B. Volochine, in *Battelle Institute Materials Science Colloquium 5th 1971* edited by R. E. Mills (McGraw-Hill, New York, 1971), pp. 529–540.
[5] M. G. D. Beysens and B. Moncef-Bouanz, Phys. Rev. A **28**, 2491 (1983).
[6] A. Dobbertin, Ph.D. thesis, Martin Luther University, 1996 (unpublished).
[7] C. S. Bak and W. I. Goldburg, Phys. Rev. Lett. **2**, 1218 (1969).
[8] W. I. G. C. S. Bak and P. N. Pusey, Phys. Rev. Lett. **25**, 1430 (1970).

[9] M. E. Fisher, Phys. Rev. **176**, 257 (1968).
[10] M. E. Fisher and P. E. Scesney, Phys. Rev. A **2**, 825 (1970).
[11] B. Chu and F. L. Lin, J. Chem. Phys. **61**, 5132 (1974).
[12] L. S. Ornstein and F. Zernike, Proc. Acad. Sci. Amsterdam **17**, 793 (1914).
[13] A. Einstein, Ann. Phys. (Leipzig) **33**, 1275 (1910).
[14] M. E. Fisher, Rep. Prog. Phys. **1**, 615 (1967).
[15] J. C. Gillou and J. Zinn-Justin, Phys. Rev. Lett. **39**, 95 (1977).
[16] L. B. J. Schmitz and D. Woermann, Ann. Phys. (Leipzig) **3**, 1 (1994).
[17] L. Landau and G. Placzek, Phys. Z. Sowjetunion **5**, 172 (1934).
[18] K. Kawasaki, Phys. Lett. **30A**, 325 (1969).
[19] L. P. Kadanoff and J. Swift, Phys. Rev. **89**, 166 (1968).
[20] R. A. Ferrell, Phys. Rev. Lett. **24**, 1169 (1970).
[21] P. T. J. Rouch and S. Chen, Phys. Rev. A **25**, 448 (1982).
[22] E. Anglescu and S. Zinca, Bull. Sect. Sci. Acad. Roum. **24**, 106 (1942).
[23] W. P. Kao and B. Chu, J. Chem. Phys. **50**, 3896 (1969).
[24] G. Golub and V. Pereyra, SIAM (Soc. Ind. Appl. Math.) J. Numer. Anal. **10**, 414 (1973).
[25] M. Osborne, in *Numerical Methods for Non-Linear Optimizations*, edited by F. A. Lootsma (Academic, London, 1972).
[26] S. W. Provencher, J. Chem. Phys. **64**, 2772 (1976).
[27] R. Griffiths and J. Wheeler, Phys. Rev. A **2**, 1047 (1970).